Laser and Particle Beams (2017), *35*, 304–312.

doi:10.1017/S0263034617000192

Heating in ultraintense laser-induced shock waves

SHALOM ELIEZER,[1] SHIRLY VINIKMAN PINHASI,[3] JOSÉ MARIA MARTINEZ VAL,[1] EREZ RAICHER,[2,4] AND ZOHAR HENIS[2]

[1]Nuclear Fusion Institute, Polytechnic University of Madrid, Madrid, Spain
[2]Applied Physics Division, Soreq NRC, Yavne, Israel
[3]Private Residence, Rehov Beeri 62, Rehovot, Israel
[4]Racah Institute of Physics, Hebrew University, Jerusalem, Israel

(Received 20 January 2017; Accepted 20 February 2017)

Abstract

This paper considers the heating of a target in a shock wave created in a planar geometry by the ponderomotive force induced by a short laser pulse with intensity higher than 10^{18} W/cm^2. The shock parameters were calculated using the relativistic Rankine–Hugoniot equations coupled to a laser piston model. The temperatures of the electrons and the ions were calculated as a function of time by using the energy conservation separately for ions and electrons. These equations are supplemented by the ideal gas equations of state (with one or three degrees of freedom) separately for ions and electrons. The efficiency of the transition of the work done by the laser piston into internal thermal energy is calculated in the context of the Hugoniot equations by taking into account the binary collisions during the shock wave formation from the target initial condition to the compressed domain. It is shown that for each laser intensity there is threshold pulse duration for the formation of a shock wave. The explicit calculations are done for an aluminum target.

Keywords: Intense lasers; Laser piston model; Shock waves

1. INTRODUCTION

The interaction of a high-intensity laser with a planar solid target may generate a one-dimensional (1D) shock wave (Eliezer, 2002, 2013; Fortov & Lomonosov, 2010). For non-relativistic intensities, 10^{12} W/cm^2 $< I_L <$ 10^{16} W/cm^2 and nanosecond pulse duration, the absorption of the laser energy results in large increase of the plasma temperature and the ablation pressure induces a strong shock wave moving into the interior of the target. For laser intensities $I_L > 10^{18}$ W/cm^2 the laser ponderomotive force pushes electrons ahead, so that the charge separation field forms a double layer (DL), in which the ions are accelerated forward. This DL structure, called a laser piston, drives a shock/compression wave moving in the unperturbed plasma. The DL separates the propagation path of the laser pulse from the shocked plasma. This plasma has in general different ion and electron temperatures. The structure of the piston and the relation between its velocity and the laser intensity were described analytically and as well obtained in particle-in-cell (PIC) simulations (Esirkepov *et al.*, 2004; Naumova *et al.*, 2009; Schlegel *et al.*, 2009; Eliezer *et al.*, 2014; Eliezer *et al.*, 2016; Schmidt & Boine-Frankenheim, 2016). The laser piston as a mechanism of particle acceleration to relativistic velocities was described in papers by Robinson *et al.* 2009 and Macchi, 2013 and references therein. Two fluid simulations of laser–plasma interaction where the nonlinear pondermotive force was dominant predicted ultrahigh acceleration of plasma blocks (Hora, 2012).

In this paper, we consider the shock wave induced by the laser piston propagating into the material, in particular the heating of the material produced during the shock compression. Section 2 presents the relativistic Rankine–Hugoniot equations describing the shock wave in the material and the dependence of the shock parameters on the laser intensity. Section 3 proposes a model of the plasma heating produced during the laser piston-induced shock wave, Section 4 presents numerical results, and Section 5 concludes the paper.

2. LASER PISTON-INDUCED RELATIVISTIC SHOCK WAVE

The shock wave induced by the laser piston is described by the relativistic Rankine–Hugoniot equations, relating the shock pressure P, energy density e, mass density ρ, particle

Address correspondence and reprint requests to: Z. Henis, E-mail: ZoharHenis@gmail.com

(piston) velocity u_p, and shock velocity u_s. The quantities with subscript zero are the corresponding material parameters before the shock arrival:

$$\frac{u_p}{c} = \sqrt{\frac{(P-P_0)(e-e_0)}{(e_0+P)(e+P_0)}}, \tag{1a}$$

$$\frac{u_s}{c} = \sqrt{\frac{(P-P_0)(e+P_0)}{(e-e_0)(e_0+P)}}, \tag{1b}$$

$$\frac{(e+P)^2}{\rho^2} - \frac{(e_0+P_0)^2}{\rho_0^2} = (P-P_0)\left[\frac{(e_0+P_0)}{\rho_0^2} + \frac{(e+P)}{\rho^2}\right], \tag{1c}$$

where c is the speed of light.

The relativistic shock wave of Eq. (1) yields the following non-relativistic well-known Hugoniot equations, when the velocities v satisfy $v/c \ll 1$, and $e = \rho c^2 + \rho E$, where P and ρE are much smaller than ρc^2:

$$u_p = \left(\frac{1}{\rho_0} - \frac{1}{\rho}\right)^{1/2} (P-P_0)^{1/2}, \tag{2a}$$

$$u_s = \frac{1}{\rho_0}\left(\frac{1}{\rho_0} - \frac{1}{\rho}\right)^{-1/2} (P-P_0)^{1/2}, \tag{2b}$$

$$E - E_0 = \frac{1}{2}\left(\frac{1}{\rho_0} - \frac{1}{\rho}\right)(P+P_0). \tag{2c}$$

We assume an ideal equation of state (EOS)

$$e = \rho c^2 + \frac{P}{\Gamma - 1}, \tag{3}$$

where c is the velocity of light and $\Gamma = c_p/c_v$ is the specific heat ratio related to the number of degrees of freedom per particle f by $\Gamma = 1 + 2/f$. In most of the calculations presented here, we assume that the specific heat ratio is, $\Gamma = 5/3$, $f = 3$. In the non-relativistic limit, the above EOS is $E = \dfrac{P}{\rho(\Gamma - 1)}$.

The laser piston velocity u_p, or $\beta_p = u_p/c$, as a function of the laser intensity I_L can be obtained by solving the relativistic Rankine–Hugoniot equations together with the piston model equation:

$$P = \frac{2I_L}{c}\frac{1-\beta_p}{1+\beta_p}, \tag{4}$$

where P is the radiation pressure equal to the shock pressure (Eliezer *et al.*, 2014).

It is convenient to solve the relativistic Rankine–Hugoniot equations in dimensionless units: compression, $\kappa = \rho/\rho_0$, dimensionless pressure $\Pi = P/\rho_0 c^2$, and dimensionless laser intensity $\Pi_L = I_L/\rho_0 c^3$ (Eliezer *et al.*, 2014). For example, for aluminum, the material considered here, the initial density $\rho_0 = 2.7\ \mathrm{g/cm^3}$, the pressure is obtained by multiplying the dimensionless pressure by $\rho_0 c^2 = 2.43 \times 10^9$ Mbar, and the laser intensity by multiplying the dimensionless intensity by $\rho_0 c^3 = 7.29 \times 10^{24}\ \mathrm{W/cm^2}$.

Substituting the ideal EOS [Eq. (3)] into the Rankine–Hugoniot Eq. (2), we obtain the relativistic Hugoniot equation:

$$\Pi^2 + B\Pi + C = 0, \tag{5}$$

$$\Pi = \frac{-B + \sqrt{B^2 - 4C}}{2}, \tag{6}$$

$$B = \frac{(\Gamma-1)^2}{\Gamma}(\kappa_0\kappa - \kappa^2) + \Pi_0(\Gamma - 1)(1 - \kappa^2), \tag{7}$$

$$C = \frac{(\Gamma-1)^2}{\Gamma}(\kappa - \kappa_0\kappa^2)\Pi_0 - \kappa^2\Pi_0^2). \tag{8}$$

Similarly, the non-relativistic Hugoniot Eq. (3a) can be written as:

$$\Pi = \frac{\kappa\kappa_0 - 1}{\kappa_0 - \kappa}\Pi_0. \tag{9}$$

In equations (7) and (8), $\kappa_0 = (\Gamma + 1)/(\Gamma - 1)$ is the non-relativistic asymptotic compression in the limit of infinite shock pressure.

We consider here the transition between the relativistic and non-relativistic regimes:

$$10^{-9} \le \Pi \le 10^{-2}. \tag{10}$$

The laser intensities that we consider here in the above transition domain lead to piston and shock velocities that are non-relativistic. However, for the high pressure obtained due to the laser pressure, the compression is slightly higher than κ_0, the asymptotic non-relativistic limit, and the non-relativistic Rankine–Hugoniot Eq. (9) does not have solution in this regime. Therefore, we must solve the relativistic Hugoniot Eq. (5) coupled to the laser piston relation (4).

In the transition domain Eqs (3a, 3b), for $u_p/c < 0.03$ lead to the following expressions for the particle and shock velocities:

$$\frac{u_p}{c} = \sqrt{\frac{2\Pi}{\Pi + 1}}, \tag{11a}$$

$$\frac{u_s}{c} = \sqrt{\frac{(\Gamma+1)\Gamma}{2}}. \tag{11b}$$

Figures 1 and 2 display the compression as a function of the dimensionless pressure for relativistic shock waves for two ideal gas EOS, $\Gamma = 5/3$ and $\Gamma = 3$, respectively, obtained by solving the Hugoniot equations. These graphs hold

https://doi.org/10.1017/S0263034617000192 Published online by Cambridge University Press

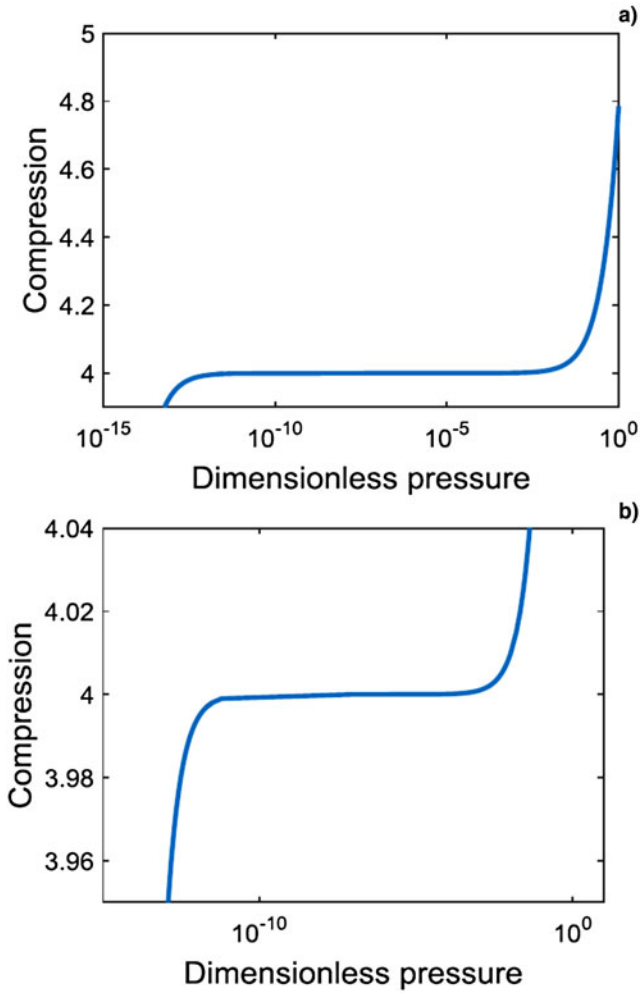

Fig. 1. (a) The compression $\kappa = \rho/\rho_0$ as a function of the normalized, dimensionless pressure, $\Pi = P/\rho_0 c^2$, for $\Gamma = 5/3$. For aluminum, $\rho_0 c^2 = 2.43 \times 10^9$ Mbar. (b) Zoom in Fig. 1a for the semi-relativistic case.

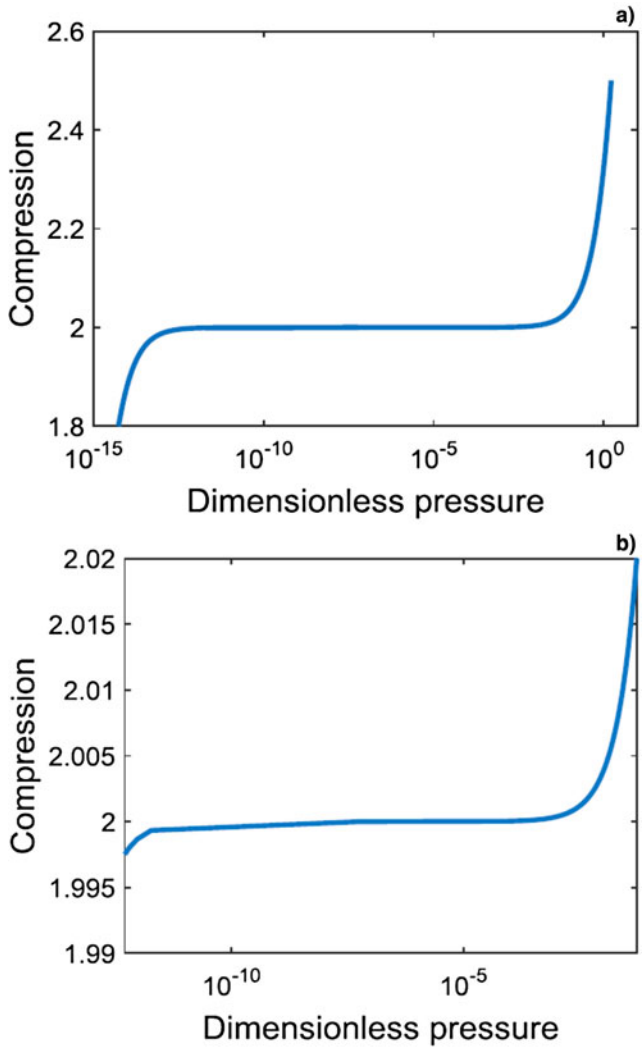

Fig. 2. (a) The compression $\kappa = \rho/\rho_0$ as a function of the normalized, dimensionless pressure, $\Pi = P/\rho_0 c^2$, for $\Gamma = 3$. (b) Zoom in Fig. 2a for the semi-relativistic case.

generally for relativistic shock waves and are not dependent on the laser piston model considered here. Figures 1b and 2b are zooms of Figures 1a, and 2a, enhancing the transition domain between non-relativistic and relativistic regimes.

Figures 3 and 4, show the particle and the shock velocities as a function of the laser intensity, for $\Gamma = 5/3$ and $\Gamma = 3$, respectively. Figures 3b and 4b zoom into Figure 3a and 3b, showing the transition regime. We note the difference between the relation between the particle and shock velocity between the two cases.

Owing to the shock wave formation in the material, the ions and the electrons behind the shock front are moving with the piston velocity u_p. For non-relativistic, and/or nanosecond or longer time duration shock waves the piston work is divided equally to kinetic energy $\int \rho u_p^2/2\, dV$ and increase in internal/thermal energy $\int 3/2 k_B (n_e T_e + n_i T_i) dV$ (Zeldovich & Raizer, 1966). The shocked plasma has in general different ion and electron temperatures, T_i and T_e (Eliezer *et al.*, 2015). However, for extremely short laser pulse duration and high laser intensity, the ions might not have enough time to achieve thermalization among themselves or with the electrons during the shock duration and the laser piston work may be partitioned differently between kinetic and internal energy. In this paper, we address this issue, estimating the time of temperature equilibration among the ions and the time of temperature equilibration between the electrons and the ions. It will be shown that for given laser intensity there is a threshold pulse duration for formation of a shock wave. In addition, dependent on the laser intensity, the electrons and ions temperature at the end of the pulse duration may be different.

3. MODEL OF THERMALIZATION IN LASER-INDUCED SHOCK WAVES

The time-dependent equations for the electrons and ions temperatures T_e and T_i are obtained from the energy conservation

https://doi.org/10.1017/S0263034617000192 Published online by Cambridge University Press

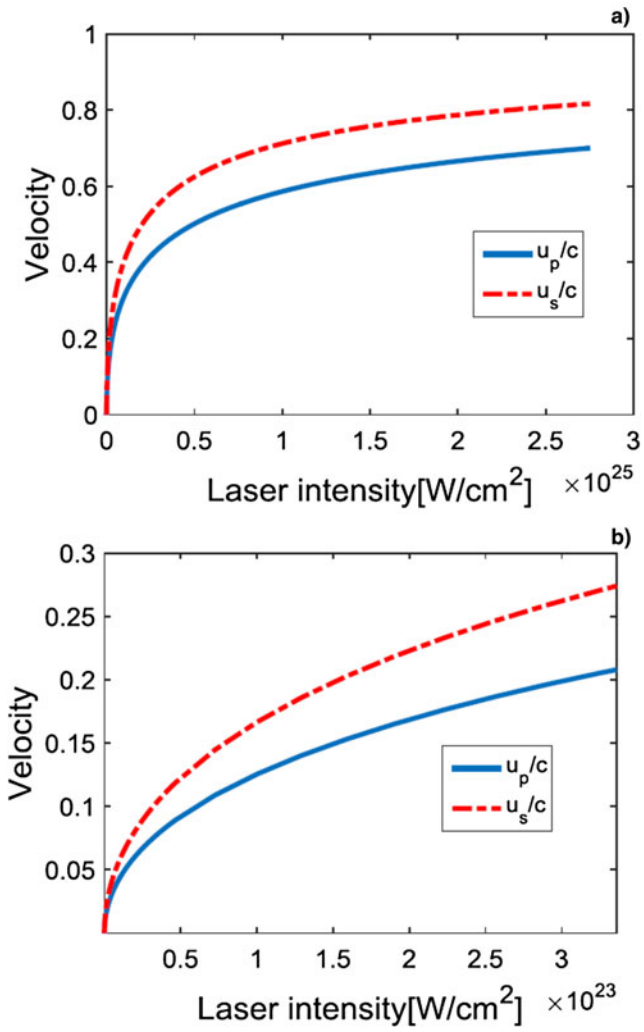

Fig. 3. The particle and the shock velocities as a function of the laser intensity, for $\Gamma = 5/3$. (b) Zoom in Fig. 3a for the semi-relativistic case.

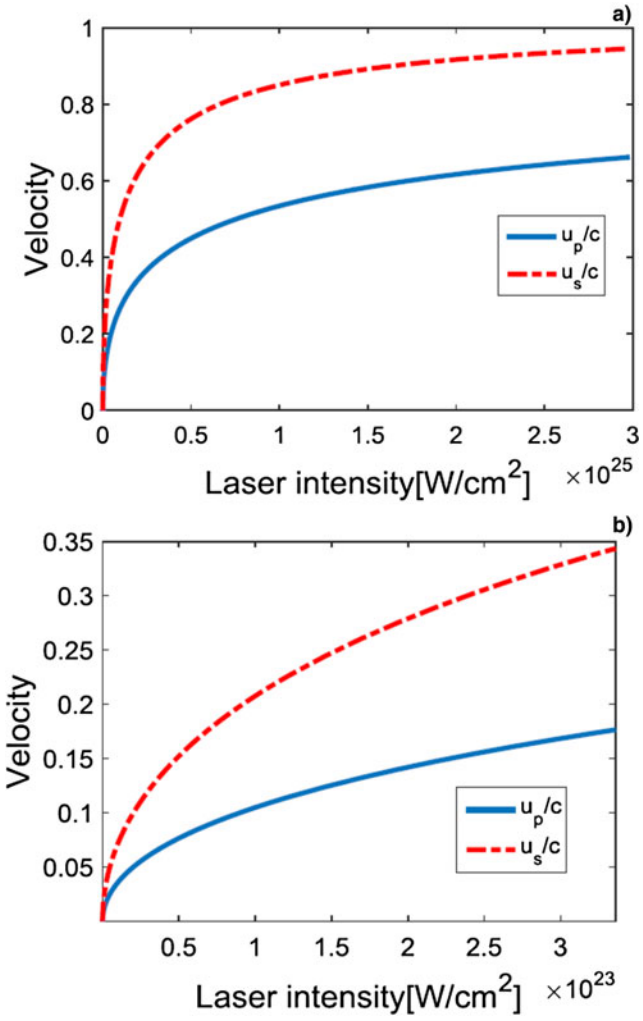

Fig. 4. The particle and the shock velocities as a function of the laser intensity, for $\Gamma = 3$. (b) Zoom in Fig. 3a for the semi-relativistic case.

of the electrons and the ions:

$$\frac{d}{dt}\left(\frac{3}{2}n_e k_B T_e\right) = W_{ie} - W_B + W_d^e f_{ee} + W_d^i f_{ie}, \quad (12)$$

$$\frac{d}{dt}\left(\frac{3}{2}n_i k_B T_i\right) = -W_{ie} + W_d^e f_{ei} + W_d^i f_{ii}. \quad (13)$$

The electrons and ions densities are n_e and n_i, and k_B is the Boltzmann constant. $W_{ie}[\mathrm{erg/cm^3/s}]$ is the rate of the electron-ion exchange energy density and $W_B[\mathrm{erg/cm^3/s}]$ is the appropriate bremsstrahlung losses of the electron energy density. The power rate deposition into the ions W_d^i and the electrons W_d^e are obtained from the piston work. This energy is deposited only in part into the thermal energy and the factors f_{ij} (i,j = e or i) are describing the efficiency of this energy deposition. It is important to point out that the upper limit of $W_d^i + W_d^e$ equals 50% of the piston energy density rate.

The bremsstrahlung power loss term is:

$$W_B\left[\frac{\mathrm{erg}}{\mathrm{cm^3/s}}\right] = 1.25\times10^{-25} n_e n_i Z_{av}^2 T_e^{0.5}\left(1 + \frac{2T_e}{0.511\times10^6}\right). \quad (14)$$

Here the electron temperature is in eV units and Z_{av} is the average ionization in the material.

The temperature equilibration term between the electrons and the ions is:

$$W_{ie}\left[\frac{\mathrm{erg}}{\mathrm{cm^3/s}}\right] = \frac{3}{2}n_e k_B \frac{(T_i - T_e)}{\tau_{eq}}. \quad (15)$$

The electron ion thermal equilibration time τ_{eq}, is given by:

$$\tau_{eq} = \frac{3m_e m_i}{8(2\pi)^{1/2}}\frac{1}{n_i Z_{av}^2}\frac{1}{e^4 \ln\Lambda}\left(\frac{k_B T_e}{m_e} + \frac{k_B T_i}{m_i}\right)^{3/2}, \quad (16)$$

where m_e and m_i are the electron and ion masses and e is the electron charge.

https://doi.org/10.1017/S0263034617000192 Published online by Cambridge University Press

From the fact that 50% of the piston work can contribute to the thermal energy we obtain

$$W_{\rm d}\left[\frac{\rm erg}{\rm cm^3/s}\right]=\frac{Pu_{\rm p}}{2(u_{\rm s}-u_{\rm p})\tau_{\rm L}}-\frac{1}{\tau_{\rm L}}\int W_{\rm B}dt, \tag{17}$$

where the laser pulse duration is $\tau_{\rm L}$. Using further the non-relativistic Hugoniot conservation Eq. (3) one has

$$\frac{Pu_{\rm p}}{2(u_{\rm s}-u_{\rm p})\tau_{\rm L}}=\frac{\rho u_{\rm p}^2}{2\tau_{\rm L}}. \tag{18}$$

The deposition rate $W_{\rm d}$ is calculated after solving the Hugoniot relativistic equations for the pressure and the particle and shock velocities as a function of the laser intensity.

We consider the energy deposition to the electrons and the ions, as test particles and as field particles, separately.

$$W_{\rm d}^{\rm i}=\frac{W_{\rm d}}{(1+n_{\rm e}m_{\rm e}/n_{\rm i}m_{\rm i})}, \tag{19}$$

$$W_{\rm d}^{\rm e}=W_{\rm d}-W_{\rm d}^{\rm i}, \tag{20}$$

$$W_{\rm d}\left[\frac{\rm erg}{\rm cm^3/s}\right]=\frac{\rho u_{\rm p}^2}{2\tau_{\rm L}}-\frac{1}{\tau_{\rm L}}\int W_{\rm B}dt. \tag{21}$$

Here $m_{\rm i}$ and $m_{\rm e}$ are the ion and electron masses, and $n_{\rm i}$ and $n_{\rm e}$ are the ions and electrons densities. Owing to the larger ion mass, $W_{\rm d}^{\rm i}\gg W_{\rm d}^{\rm e}$.

Assuming that the laser pulse rise time is very small in comparison with the laser pulse duration, we get at the shock wave surface an instant change of target particles from zero to a velocity $u_{\rm p}$. This is equivalent to a shock wave rise time much shorter than the laser pulse duration. We assume that the time equilibrations to reach the instant temperatures $T_{\rm e}(t<\tau_{\rm L})$ and $T_{\rm i}(t<\tau_{\rm L})$ are obtained by collisions near the shock wave front. In this model, we describe the piston energy deposition of the shocked particles, electrons and ions into thermal energy using a relaxation rate arising from interaction of test particles, labeled α, streaming with velocity $u_{\rm p}$, through a background of field particles, labeled β with a collision frequency of energy deposition (Huba, 2013) given by:

$$\nu_{\varepsilon}^{\alpha/\beta}=2\left[\frac{m_\alpha}{m_\beta}\psi(x^{\alpha/\beta})-\psi'(x^{\alpha/\beta})\right]\nu_0^{\alpha/\beta}. \tag{22}$$

Here α and β stand for the electrons or ions and α/β denotes the kinetic energy transferred from test α to field β particles, m stands for the electrons and ion mass. $\nu_0^{\alpha/\beta}$, the relaxation rate scale and the function ψ are defined by:

$$\nu_0^{\alpha/\beta}=4\pi q_\alpha^2 q_\beta^2\lambda_{\alpha\beta}n_\beta/m_\alpha^2v_\alpha^3, \tag{23}$$

$$x^{\alpha/\beta}=\frac{m_\beta v_\alpha^2}{2k_{\rm B}T_\beta}, \tag{24}$$

$$\psi(x)=\frac{2}{\pi}\int_0^x dtt^{1/2}e^{-t}\,, \tag{25}$$

$$\psi'(x)=\frac{d\psi}{dx}. \tag{26}$$

T_β denotes the temperature of the field particles, v is the test particles velocity, $v=u_{\rm p}$, q_α, and q_β are the charges (q equals the electron charge e for the electrons and $Z_{\rm av}$ e for the ions), and $k_{\rm B}$ is the Boltzmann constant. $\lambda_{\alpha\beta}=\ln\Lambda_{\alpha\beta}$ is the Coulomb logarithm. The transfer rate $\nu_\varepsilon^{\alpha/\beta}$ is positive for $\varepsilon>\varepsilon_\alpha^*$, and negative for $\varepsilon<\varepsilon_\alpha^*$, where $\varepsilon=1/2m_\alpha v_\alpha^2$ and $x^*=(m_\beta/m_\alpha)(\varepsilon_\alpha^*/T_\beta)$ is the solution of $\hat{\psi}'(x^*)=m_\alpha/m_\beta\psi(x^*)$.

The factors f account for the relaxation rates of energy deposition and are defined by:

$$f_{\rm ee}=\min(t\cdot\nu_\varepsilon^{\rm e/e},1), \tag{27a}$$

$$f_{\rm ei}=\min(t\cdot\nu_\varepsilon^{\rm e/i},1), \tag{27b}$$

$$f_{\rm ie}=\min\,(t\cdot\nu_\varepsilon^{\rm i/e},1), \tag{27c}$$

$$f_{\rm ii}=\min\,(t\cdot\nu_\varepsilon^{\rm i/i},1). \tag{27d}$$

The average ionization $Z_{\rm av}$ is obtained from the calculation of population of the ionization stages as a function of time:

$$\frac{dn_z}{dt}=n_{\rm e}(n_{z-1}S_z-n_zS_{z+1}-n_zR_z+n_{z+1}R_{z+1}), \tag{28}$$

where S_z is the ionization coefficient for creating an ion with charge z, R_z is the recombination coefficient of an ion with of charge z, and $n_{\rm e}=\sum_{z=1}^{Z}zn_z$ is the electron density, Z is the atomic number.

The following analytical expressions for the ionization and recombination rates were used (Eidmann, 1994):

$$S_z=2.4\times10^{-6}\Delta_z\frac{T_{\rm e}^{1/4}}{I_z^{7/4}}e^{-I_z/T_{\rm e}}\left[\frac{\rm cm^3}{\rm s}\right], \tag{29}$$

where I_z[eV] is the ionization potential of an ion with charge z, Δ_z is the number of electrons in the last occupied shell of the ion with charge z.

The recombination rate is generally the contribution of three body and radiative recombination:

$$R_{z+1}^3=3.9\times10^{-28}\frac{\xi_{z+1}}{I_Z^{7/4}T_{\rm e}^{5/4}}\left[\frac{\rm cm^6}{\rm s}\right], \tag{30}$$

https://doi.org/10.1017/S0263034617000192 Published online by Cambridge University Press

$$R^{r}_{z+1} = 1.9\times10^{-14}\frac{I_z}{T_e^{1/2}}\left[\frac{\mathrm{cm}^3}{\mathrm{s}}\right]. \quad (31)$$

Here ξ_{z+1} is the number of vacancies in the last shell of ion z. In the above ionization and recombination rates T_e is in eV units.

The $(Z+1)$ equations for the ionization states, (including the neutral) are solved together with the ions and electron temperatures as a function of time.

4. NUMERICAL RESULTS

We consider the following two cases of laser piston-induced shock waves, with different laser intensities, corresponding to piston velocities u_p, 0.001 and $0.01c$. We consider the following constrains on the laser spot size and pulse duration. First, a lower limit on the spot size is set by the diffraction limit, $r_L = r_{DL} = 1.22\,\lambda_L \approx 1$ μm, where r_L is the spot radius and $\lambda_L = 0.8$ μm is the laser wavelength. Secondly, to obtain a 1D shock wave, the spot size must be larger than l_s the spatial scale of the shocked region:

$$2\cdot r_L > l_s, \quad (32)$$

$$l_s = (u_s - u_p)\cdot\tau_L\,. \quad (33)$$

In Eq (33), τ_L is the laser pulse duration. In the calculations here where we assume that the laser spot radius is given by $r_L = 1.5\cdot l_s$. Thirdly, formation of a shock wave requires that the spatial scale of shocked region is larger than the spatial scale of the shock front width:

$$(u_s - u_p)\cdot\tau_L \gg \tau_R u_s, \quad (34)$$

where is

$$\tau_R = \max(\tau_e, \tau_i), \quad (35)$$

$$\tau_e = \frac{1}{\nu_e^{e/e} + \nu_e^{e/i}}, \quad (36)$$

$$\tau_i = \frac{1}{\nu_i^{i/e} + \nu_i^{i/i}}. \quad (37)$$

In the calculations, we approximate Eq. (34) as $(u_s - u_p)\cdot\tau_L = 3\cdot\tau_R u_s$. This condition and Eq. (11) leads for $\Gamma = 5/3$, $\tau_L = 12\tau_R$.

The values for the piston velocity 0.001 and 0.01 correspond to laser intensities I_L: 4.87×10^{18} and 4.95×10^{20} W/cm^2, in the transition domain between non-relativistic and relativistic regimes. We assume normal density of aluminum $\varrho_0 = 2.7$ g/cm^3 and $\Gamma = 5/3$. The piston, or particle velocity, u_p and shock wave velocity, u_s, as well as the shock pressure, compressibility are calculated as a function of the laser intensity, and are given in Table 1, for $\Gamma = (5/3)$. The required laser energy can be estimated as $E_L = I_L\pi r_L^2\tau_L$.

Figure 5 shows the results of the equations for the low laser intensity considered here, corresponding to $u_p = 0.001\ c$. In this case, $r_L \approx r_{DL} \approx 1.5 l_s$ for pulse duration $\tau_L = 6.5$ ps. It is shown below that the constrain (34) applies as well. The simulation is done for a time equal to the laser pulse duration, 6.5 ps, for this case. The electrons and ions temperatures as a function of time are shown in Figure 5a. Apart from at very early times, the ions temperature is higher than the electrons temperature by few tens percent. Both temperatures increase with time until about 2.7 ps, then, the ions temperature starts decreasing due to energy transfer to the electrons. Shortly after that, the ions and electron temperatures become equal, and the plasma is cooling due to bremsstrahlung losses. The electrons and ions thermal energy, $3/2\ n_e k_B T_e$ and $3/2\ n_i k_B T_i$, as well as the bremsstrahlung loss $\int W_B dt$, as a function of time are shown in Figure 5b. Owing to the larger electron density, the electron thermal energy is larger. The temperature equilibration term between the ions and the electrons W_{ie} is negative at early times, as at these times the kinetic energy is deposited into the electrons and their temperature is higher than the ion temperature, and afterwards becomes positive as the thermal energy flow goes from the ions to the electrons. The bremsstrahlung losses increase as the electrons temperature increases and then decreases when the temperature starts descending. The four energy transfer rates, $\nu_e^{\alpha/\beta}$, where α and β denote the electrons or the ions, are displayed in Figure 5c. In order to plot all the four rates on the same plot, since the rates may change sign, according to the possibility to release energy or gain energy, we display for all the cases absolute values of the transfer rates. The two upper curves stand for the rates of the energy transfer from the electrons to the electrons and the ions, which are higher by three to six orders of magnitude than the energy transfer rates from the ions. However, the kinetic energy of the electrons is smaller by more than three orders of magnitude than the ions energy. The two lower curves

Table 1. *The laser and shock wave parameters of two laser piston-induced shock waves, calculated with $\Gamma = 5/3$.*

	$u_p = 0.001c$	$u_p = 0.01c$
Pressure P[erg/cm^3]	3.38×10^{15}	3.24×10^{17}
Normalized pressure Π	1.39×10^{-6}	1.33×10^{-4}
Density ratio $\kappa = \varrho/\varrho_0$	4.0000013	4.000125
$u_s[c]$	0.0013	0.0133
Laser intensity I_L[W/cm^2]	5.082×10^{18}	4.95×10^{20}
Normalized laser intensity Π_L	6.971×10^{-7}	6.8×10^{-5}
Laser pulse duration τ_L[ps]	6.5	12
Deposition rate W_d[erg/cm^3/s]	1.5605×10^{27}	8.1×10^{28}
$\gamma = 1/\sqrt{1-u_p^2/c^2}$	1	1.0001
Laser energy $E_L[J]$	0.94	6.10^4

https://doi.org/10.1017/S0263034617000192 Published online by Cambridge University Press

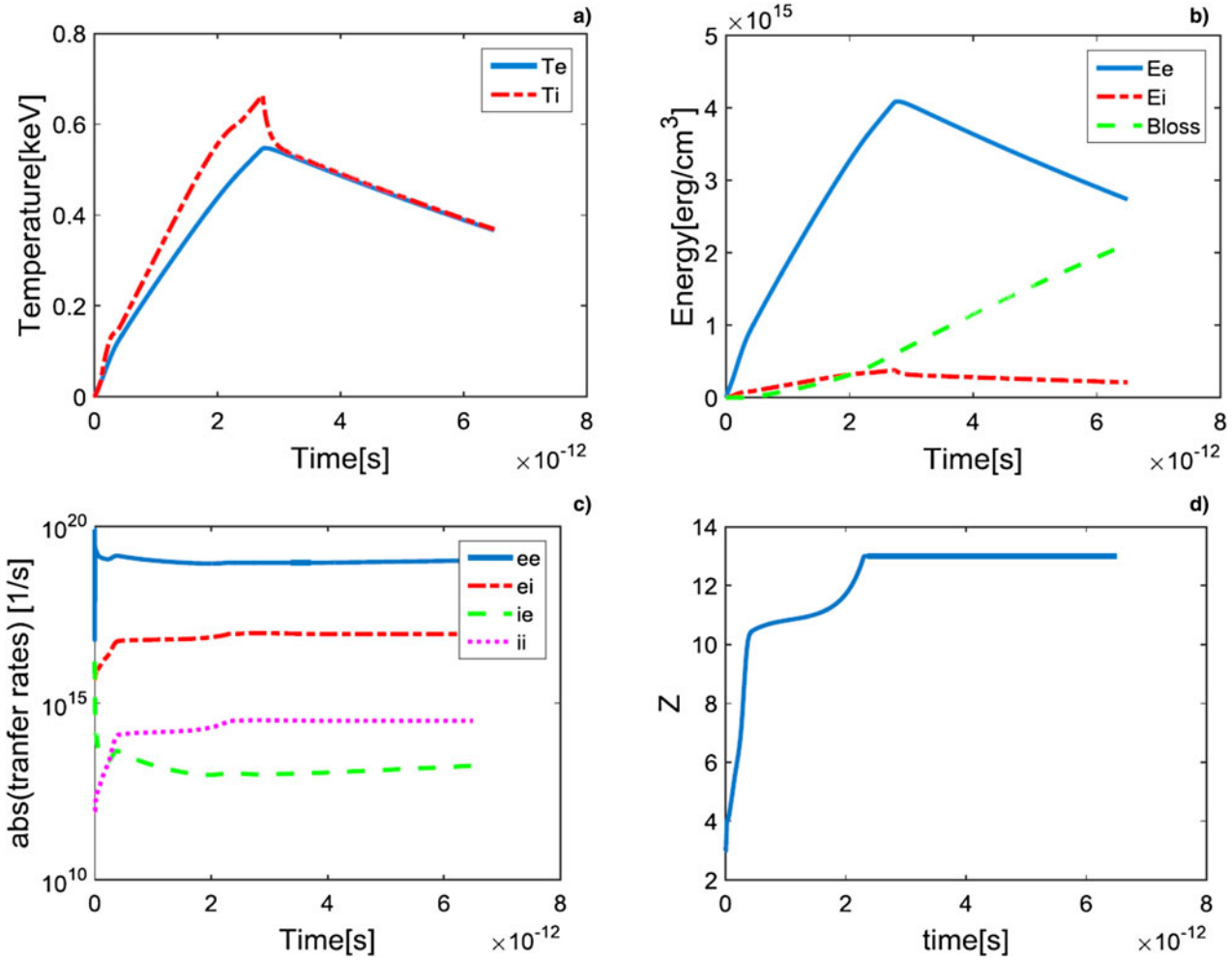

Fig. 5. Numerical results for $u_p = 0.001c$, corresponding to the lowest laser intensity considered, $I_L = 4.97 \times 10^{18}$ W/cm^2, pulse duration 6.5 ps and $\Gamma = 5/3$: (a) Electron (solid) and ion (dashed dot) temperatures as a function of time. (b) Thermal energy density of the ions, $3/2\, n_i k_B T_i$ (dashed dot), and of the electrons, $3/2\, n_e k_B T_e$ (solid), and the bremsstrahlung loss $\int_0^t W_B dt$ (dashed), as a function of time. (c) Absolute value of the energy transfer rates $\nu_\varepsilon^{\alpha/\beta}$, e/e – solid, e/I – dashed dot, i/e – dashed, and i/i – dot. (d) The average ionization as a function of time.

show the transfer rates of the ions kinetic energy to electrons and ions. The transfer rate to the ions is larger by two orders of magnitude than the transfer rate to the electrons. It is seen in Figure 5c that the relaxation time defined by Eq. (35) is of the order of 10^{-14} s, much smaller that the laser pulse duration, enabling formation of a stable shock wave.

Finally, the average ionization as a function of time is shown in Figure 5d. The slope of the average ionization curve decreases at the onset of *K*-shell ionization. Fully ionization is obtained after 2.1 ps. The energy balance for this case is the following: at the end of the laser pulse the kinetic energy of the plasma represents 50% of the piston work, the thermal energy is 29% of the piston work and the bremsstrahlung loss is 21% of the piston work. This energy partition is different than the energy partition in classical shock waves where bremsstrahlung losses are neglected, where 50% of the shock wave energy is deposited in kinetic energy and 50% in thermal energy. Thermalization between the ions and electrons occurs after 2.7 ps, a time scale of the order of the laser pulse duration. The ions temperature at the end of the deposition of the piston work is nearly the shock temperature $T_H = 0.63$ keV calculated from the pressure given by Hugoniot relations, for fully ionized aluminum and ideal EOS. By the end of the laser pulse the ions and electrons temperatures $T_i = T_e$ decrease, related to bremsstrahlung losses, leading to a decrease in the pressure comparing to the initial pressure.

Figure 6 displays the results of the calculation for the second case, with particle velocity $u_p = 0.01c$. The laser pulse time duration is determined following Eq. (32). From Eq. (23) it is seen that the relaxation rate scale scales as $1/u_p^3$. Therefore, for particle velocity ten times larger than the previous case, it is expected that the relaxation time to be in the picosecond range. Figure 6 shows results for $\tau_L = 12$ ps. At the beginning of the laser pulse the electrons heat up before the ions, however after about 300 fs, the ions temperature becomes larger

https://doi.org/10.1017/S0263034617000192 Published online by Cambridge University Press

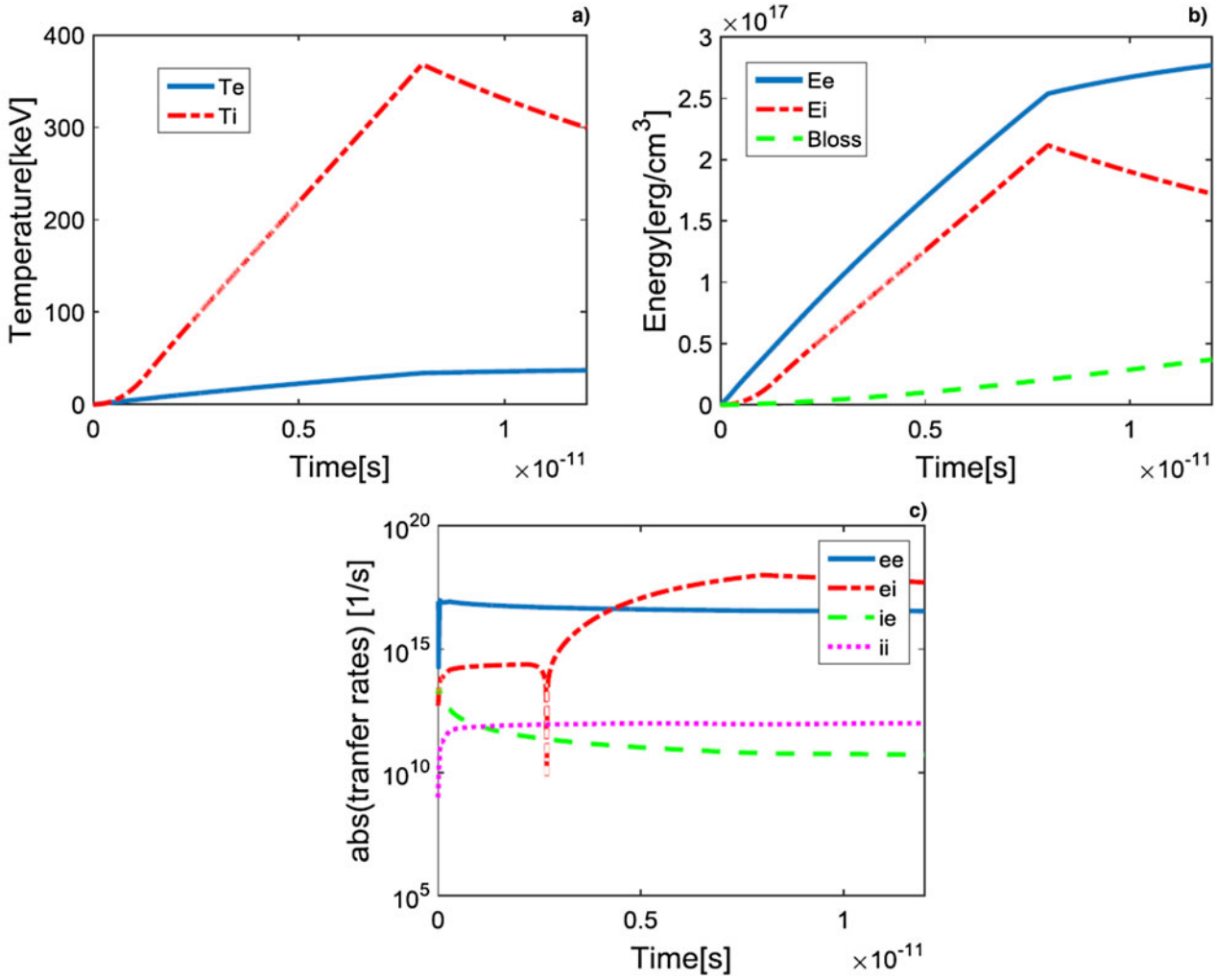

Fig. 6. Numerical results for $u_p = 0.01c$, corresponding to $I_L = 4.95 \times 10^{20}$ W/cm^2, pulse duration 12 ps and $\Gamma = 5/3$: (a) Electron (solid) and ion (dashed dot) temperatures as a function of time. (b) Thermal energy density of the ions, $3/2\, n_i k_B T_i$ (dashed dot), and of the electrons, $3/2\, n_e k_B T_e$ (solid), and the bremsstrahlung loss $\int_0^t W_B dt$ (dashed), as a function of time. (c) Absolute value of the transfer rates $\nu_\varepsilon^{\alpha/\beta}$, e/e – solid, e/i – dashed dot, i/e – dashed, and i/i – dot.

than the electron temperature. Figure 6a shows that at the end of the laser pulse the ions temperature is much larger than electrons temperature, the electrons as well as the ions reach equilibration among themselves, however at different temperatures. After about 8 ps, all the available piston work is deposited, the maximum ions temperature is 367 keV, and the ions start cooling down due to energy transfer to the electrons, reaching 302 keV at the end of the pulse duration. The electron temperature is 37 keV at this time. The temperature corresponding to the Hugoniot relation for an equilibrium shock wave in this case would be 60 keV, much lower than the ions temperature and higher than the electrons temperature. The total pressure at the end of the piston work deposition is nearly equal to the Hugoniot pressure. The ions and electrons thermal energy and the bremsstrahlung loss as a function of time are displayed in Figure 6b. The ions and the electrons do not reach thermalization. The piston energy partition at the end of the laser pulse in this case is 50% deposition into kinetic energy, 46.2% deposition into thermal energy, 17.7% into the ions and 28.5% into the electrons, and 3.8% into bremsstrahlung loss. Figure 6c shows the absolute values of the four transfer rates. It is seen that the ion–ion relaxation rate and the laser pulse duration obey Eq. (32). Owing to the higher particle and shock velocities and longer pulse duration, the shock spatial scale in this case is $l_s = 12$ μm, implying a spot radius of 18 μm and laser energy of 60 kJ.

Increasing the piston velocity by a factor of two and following the above constrains regarding the laser spot size and pulse duration leads the laser energy of tens of MJ, which is beyond the capabilities of future planned laser facilities.

5. SUMMARY

At domain where relativistic shocks are generated, mechanically interactions may dominate over thermal phenomena, when there is no time for thermal relaxation and expansion.

https://doi.org/10.1017/S0263034617000192 Published online by Cambridge University Press

In this paper, we considered heating of a thin solid layer with width of about 1 μm, shocked by the light pressure of a short pulse laser at relativistic intensities. We addressed here the regime of semi-relativistic shock waves, for laser intensities in the range 10^{18}–10^{23} W/cm^2. In these conditions, it was obtained that the shocked plasma has different temperatures, and depending on the laser intensity electrons and ions do not thermalize during the shock wave duration. As an example we calculate the heating of solid aluminum. Constrains on the laser spot size and pulse duration indicate that formation of 1D shock wave in aluminum initially at normal density, with laser energy up to the range of tens of kJ limit the laser intensity to few times 10^{20} W/cm^2. Two cases were considered. For the lowest laser intensity considered $\sim 5 \times 10^{18}$ W/cm^2, corresponding to particle velocity $u_p = 0.001c$, thermalization between the electrons and the ions is reached after about 3 ps at a temperature of about 0.6 keV. Increasing the laser intensity by two orders of magnitude, to $\sim 5 \times 10^{20}$ W/cm^2, there is no thermalization between the electrons and the ions, during the shock duration and a two temperature shock wave is obtained with ions temperature much higher than the electrons temperature.

We note that our results at laser intensity $\sim 5 \times 10^{20}$ W/cm^2 seem to be consistent with an experiment reported by (Akli *et al*., 2008). In their experiment, the heating of solid targets by 5×10^{20} W/cm^2, 0.8 ps, 1.05 μm wavelength laser was studied by the X-ray spectroscopy of the *K*-shell emission from thin layers of Ni, Mo, and V, and temperatures of the order of 5 keV were obtained. This temperature is consistent with the electron temperature of 37 keV, obtained in our calculations with longer pulse duration of 12 ps. In addition, PIC simulations (Denavit, 1992; Silva *et al*., 2004; Akli *et al*., 2008) reported that the longitudinal ion space shows the signature of a light pressure-driven shock with ions moving at the flow velocity of $0.015c$ behind the shock, and a smaller group of reflected ions at twice of that velocity. Moreover, in those PIC simulation, the energy density increased by more than an order of magnitude in the shock, while the particle density increased twofold, illustrating that the material was heated and compressed at the same time, characteristic to shocked material behavior.

REFERENCES

Akli, K.U., Hansen, S.B., Kemp, A.J., Freeman, R.R., Beg, F.N., Clark, D.C., Chen, S.D., Hey, D., Hatchett, S.P., Highbarger, K., Giraldez, E., Green, J.S., Gregori, G., Lancaster, K.L., Ma, T., MacKinnon, A.J., Norrey, P., Patel, J., Shearer, C., Stephens, R.B., Stoeckl, C., Storm, M., Theobald, W., Van Woerkom, L.D., Weber, R. & Key, M.H. (2008). Laser heating of solid matter by light-pressure-driven shocks at ultrarelativistic intensities. *Phys. Rev. Lett*. **100**, 165002.

Denavit, J. (1992). Absorption of high intensity subpicosecond lasers on solid density targets. *Phys. Rev. Lett*. **69**, 3052.

Eidmann, K. (1994). Radiation transport and atomic physics modeling in high energy density laser produced plasmas. *Laser Part. Beams* **12**, 223.

Eliezer, S. (2002). *The Interaction of High-Power Lasers with Plasmas*. Boca Raton, Florida: CRS press.

Eliezer, S. (2013). Shock waves and equations of state related to laser–plasma interaction, in laser–plasma interactions and applications. *68th Scottish Universities Summer School in Physics* (McKenna, P., Neely, D., Bingham, R. and Jaroszynski, D.A., Eds.), pp. 49–78. Heidelberg, Springer Publications.

Eliezer, S., Henis, Z., Nissim, N., Pinhasi, S.V. & Martinez Val, J.M. (2015). Introducing a two temperature plasma ignition in inertial confined targets under the effect of relativistic shock waves: the case of DT and pB11. *Laser Part. Beams* **33**, 577–589.

Eliezer, S., Martinez-Val, J.M., Henis, Z., Nissim, N., Pinhasi, S.V., Ravid, A., Werdiger, M. & Raicher, E. (2016). Physics and applications with laser induced relativistic shock waves. *High Power Laser Sci. Eng*. **4**, e25.

Eliezer, S., Nissim, N., Raicher, E. & Martinez Val, J.M. (2014). Relativistic shock waves induced by ultra-high laser pressure. *Laser Part. Beams* **32**, 243–251.

Esirkepov, T., Borghesi, M., Bulanov, S.V., Mourou, G. & Tajima, T. (2004). Highly efficient relativistic ion generation in the laser piston regime. *Phys. Rev. Lett*. **92**, 175003/1–4.

Fortov, V.E., Lomonosov, L.V. (2010). Shock waves and equations of state of matter. *Shock Waves* **20**, 53–71.

Hora, H. (2012). Fundamental difference between picosecond and nanosecond laser interaction with plasmas: ultrahigh plasma block acceleration links with electron collective ion acceleration of ultra-thin foils. *Laser Part. Beams* **30**, 325.

Huba, J.D. (2013). *NRL Plasma formulary*, Supported by the office of Naval Research Laboratory, Washington DC, p. 1–71.

Macchi, A. (2013). Ion acceleration by super-intense laser plasma interaction. *Rev. Mod. Phys*. **85**, 751.

Naumova, N., Schlegel, T., Tikhonchuk, V.T., Labaune, C., Sokolov, I.V. & Mourou, G. (2009). Hole boring in a DT pellet and fast-ion ignition with ultraintense laser pulses. *Phys. Rev. Lett*. **102**, 025002.

Robinson, A.P.L., Gibbon, P., Zepf, M., Kar, S., Evans, R.G. & Bellei, C. (2009). Relativistically correct hole-boring and ion acceleration by circularly polarized laser pulses. *Plasma Phys. Control. Fusion* **51**, 024004.

Schlegel, T., Naumova, N., Tikhonchuk, V.T., Labaune, C., Sokolov, I.V. & Mourou, G. (2009). Relativistic laser piston: pondermotive ion acceleration in dense plasmas using ultraintense laser pulses, Phys. *Plasmas* **16**, 083103.

Schmidt, P. & Boine-Frankenheim, O. (2016). A gas-dynamical approach to radiation pressure acceleration, Phys. *Plasmas* **23**, 063106.

Silva, L.O., Marti, M., Davies, J.R., Fonseca, R.I., Chen, C., Tsung, F.S. & Morri, B. (2004). Proton Shock acceleration in laser plasma interaction. *Phys. Rev. Lett*. **92**, 015002.

Zeldovich, Y.B. & Raizer, Y.P. (1966). *Physics of Shock Waves and High Temperature Hydrodynamic Phenomena*. New York: Academic Press Publications.

APPENDIX

The ionization potential in eV of the aluminum ion stages from the NIST Atomic Spectra database were used in the calculations are: 5.98, 18.82, 28.44, 119.99, 153.82, 190.49, 241.76, 284.64, 330.21, 398.65, 442, 2085, 2304.14.

https://doi.org/10.1017/S0263034617000192 Published online by Cambridge University Press